Journal of proteome research

Article

pubs.acs.org/jpr

A Targeted Multiplexed Proteomic Investigation Identifies Ketamine-Induced Changes in Immune Markers in Rat Serum and Expression Changes in Protein Kinases/Phosphatases in Rat Brain

Hendrik Wesseling,[†] Hassan Rahmoune,[†] Mark Tricklebank,[‡] Paul C. Guest,[†] and Sabine Bahn*[,†,§]

[†]Department of Chemical Engineering and Biotechnology, University of Cambridge, Cambridge CB2 1QT, United Kingdom

[‡]Ely Lilly and Co. Ltd, Erl Wood Manor, Sunninghill Road, Windelesham, Surrey GU20 6PH, United Kingdom

[§]Department of Neuroscience, Erasmus Medical Center Rotterdam, 3000 CA, The Netherlands

S *Supporting Information*

ABSTRACT: There is substantial interest in the *N*-methyl-D-aspartate (NMDA) receptor antagonist ketamine in psychiatric research because it exerts acute psychotomimetic and rapid antidepressant effects in rodents and humans. Here, we investigated proteomic changes in brain and serum after acute treatment of rats with ketamine using two targeted proteomic profiling methods. Multiplex immunoassay profiling of serum identified altered levels of interleukin 4, tumor necrosis factor alpha, and fibroblast growth factor 9, suggesting a link between ketamine exposure and peripheral inflammation and growth factor dysregulation. Selected reaction monitoring mass spectrometry profiling of rat brain tissue found that proteomic changes occurred in the frontal cortex and to a greater extent in the hippocampus. This involved changes in signaling kinases and proteases such as protein kinase C beta, neurochondrin (NCDN), calcineurin, extracellular signal-regulated kinsase 1 (ERK1), and mammalian target of rapamycin (MTOR). Furthermore, altered levels were found for proteins associated with neurotransmitter metabolism (mitochondrial aspartate aminotransferase, catechol *O*-methyl transferase, synaptic vesicle endo-/exocytosis (vesicle fusing ATPase (NSF), synapsin 1 (SYN1), syndapin-1 (PACN1)). Consistent with previous global proteomic studies, we confirmed known changes in mitochondrial complex I, prohibitin (PHB) and neurofilament proteins (neurofilament light chain and α-internexin (AINX)). Taken together, the proteomic changes parallel those described in human psychiatric pathology. The results will help to elucidate ketamine's mechanism of action, which will facilitate development of novel drugs for the treatment of schizophrenia and major depressive disorder.

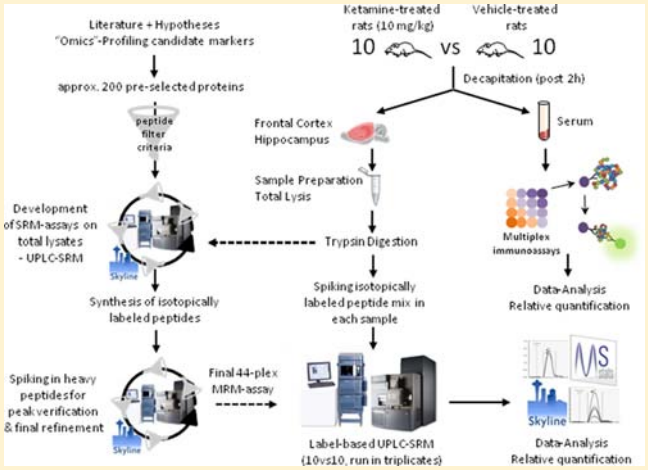

KEYWORDS: *SRM, ketamine, NMDA-receptor antagonist, major depressive disorder, schizophrenia, pharmacological treatment, MSstats, rat, multiplex immunoassay, animal model*

INTRODUCTION

Recent studies have shown that the psychosis-inducing *N*-methyl-D-aspartate (NMDA) receptor (R) antagonist ketamine also serves as a rapid-acting antidepressant, effective in treatment-resistant depression patients.[1,2] Therefore, research efforts have been rekindled to elucidate the mechanism of action of this compound. The relevance of ketamine in relation to schizophrenia is its NMDAR blocking activity, leading to hypofunction of this receptor. This is thought to induce positive symptoms of psychosis, but ketamine also blocks D_2 dopamine receptors, thus inducing negative and cognitive symptoms that have been associated with schizophrenia.[3,4] The molecular mechanisms linked to the antidepressant effect of ketamine are still under debate. An improved molecular understanding of these mechanisms could lead to the identification of novel antidepressant targets which do not have the psychotomimetic and addictive side effects of ketamine. In addition, this could also lead to novel drug targets for the treatment of the cognitive, positive and negative symptoms of schizophrenia.

Previous studies have characterized ketamine rodent models mostly at the behavioral level. These have shown effects of acute ketamine administration, such as hyperlocomotion,[5] stereotypy, impaired information processing with abnormalities in cognitive function,[6] and impaired social interaction,[7−9] which

Special Issue: Environmental Impact on Health

Received: September 10, 2014
Published: November 2, 2014

have been linked to symptoms of schizophrenia in man. In addition, behaviorally defined acute antidepressant effects of ketamine have been observed in wildtype rodents[10,11] and rodent models for major depressive disorder (MDD).[12−15] However, few studies have been performed investigating the mechanisms of action of ketamine at the physiological or molecular levels. There have been some studies that have reported effects on neurotransmitter release,[16] increased acetylcholinesterase activity,[9] dendritic branching and spine number,[10] increased neuroplasticity and synaptogenesis via enhancement of glutamatergic signaling,[10] as well as changes in immune function.[17,18] The molecular pathways that have been implicated in the ketamine response include α-amino-3-hydroxy-5-methyl-4-isoxazolepropionic acid receptor (AMPAR) signaling,[12] mammalian target of rapamycin (mTOR)-dependent synapse formation,[10,19] protein kinase C (PKC)[20] and extracellular signal-regulated kinase (ERK) signaling,[21] eukaryotic elongation factor 2 phosphorylation (p-eEF2),[22] the *Wnt*-glycogen synthase kinase (GSK-3) pathway,[23,24] oxidative stress,[25−27] and the mitochondrial respiratory chain.[25,28,29]

Here, we have investigated the acute effect of ketamine treatment in rats in the peripheral blood serum and brain tissue using a combination of targeted proteomic profiling platforms to identify which signaling molecules are involved in the mechanism of action. For this, we have used multiplex immunoassay and selected reaction monitoring mass spectrometry (SRM) platforms, two highly accurate quantitative proteomic techniques for the measurement of predetermined sets of proteins from blood serum and the brain. Although global approaches enable unbiased discovery of altered proteins via relative quantification at the proteome level, targeted techniques such as we have used here provide higher sensitivity and accuracy. Our primary objective was to generate and validate hypotheses and findings and to evaluate the potential use of this model and combined biomarker panels for future use in preclinical drug discovery and development.

MATERIALS AND METHODS

Animals

Adult R150888 Lister hooded rats (300−400g; Charles River, Margate, UK) were housed in groups of four under standard laboratory conditions with food (Harlan UK, Bicester, UK) and water available ad libitum. All experiments were conducted during the light cycle (7.00−19:00 h light phase) and were in full compliance with the Home Office Guidance (UK Animals Scientific Procedures Act 1986) and ethical policies of the Home Office. Two hours prior to sacrifice and blood sampling, rats were given a subcutaneous dose of either vehicle (0.9% sterile saline) or S(+) ketamine (10 mg/kg). Dose and pretreatment times were based on previous studies and exploratory dose/response analyses using locomotor activity ataxia, brain dialysis/neurotransmitter release and pharmacological magnetic resonance as guides to select the experimental variables.[30−33] The minimum dose was selected that gives a robust readout but low enough to avoid the induction of anesthesia. Brains were rapidly removed, rinsed in ice-cold saline and hand-dissected. The frontal cortex was defined as the anterior portion of the cortex up to 2.15 mm rostral from bregma.[34] Hippocampus was defined as the region ∼3.5−5.5 mm posterior to bregma and included dentate gyrus and CA1−3 hippocampal regions.

Serum Profiling

Rat blood samples (10 ketamine treated and 10 vehicle treated rats) were collected, and trunk blood was collected into S-Monovette 7.5 mL serum tubes (Sarstedt, Numbrecht, Germany) and left for 1.5 h at room temperature for clotting. The blood was then centrifuged at 3000*g*, 4 °C for 15 min, and the resulting supernatants (sera) were stored in low binding Eppendorf tubes (Hamburg, Germany) at −80 °C.[35]

Serum samples (90 μL) were analyzed using a rodent multianalyte profiling platform comprising multiplexed immunoassays of 89 analytes in a Clinical Laboratory Improved Amendments (CLIA)-certified laboratory at Myriad-RBM (Austin, TX, USA) as described previously.[36] Briefly, antibody−microsphere conjugates were incubated with the samples for binding of the targeted molecules. After washing, fluorescent reporter antibodies are added, which bind to different epitopes on the molecules. Unbound detection reagents were removed by washing prior to reading on a Luminex machine (Austin TX, USA). Within this instrument, the excitation beams of a red laser measured the unique fluorescent signature of each microsphere, and a green laser determined the amount of fluorescence generated in proportion to the concentration of the molecule in the sample. Data were acquired and reported in real time, affording the ability to repeatedly measure the concentration of a given molecule in each sample.

Immunoassays were calibrated using duplicate standard curves for each analyte, and raw intensity measurements were converted to protein concentrations using proprietary software. Multiplexed calibrators (eight levels per analyte) and controls (three levels per analyte) were used to monitor key performance parameters, such as lower limit of quantification, precision, cross-reactivity, linearity, spike recovery, dynamic range, matrix interference, freeze−thaw stability, and short-term sample stability, and were established for every assay as described by the manufacturer (http://www.myriadrbm.com/technology/data-quality/). Quality control samples had a coefficient of variance below 15%. Data analyses were performed using the statistical software package R (http://www.r-project.org), and the levels of analytes were determined. Analyses were conducted under blinded conditions with respect to sample identities, and samples were analyzed in random order to avoid any sequential biases. Analytes with more than 30% missing values (23 analytes) were not considered in further analysis. All remaining missing values and zero values were replaced by the half of the minimum positive value, assuming this to be the detection limit. This accounted for 1.1% of the data (14 out of 1254 data points). Furthermore, approximately 10% of the data were filtered on the basis of the relative standard deviation.[37] Row-wise normalization to each median reading was employed to adjust for differences among samples, and data were log-transformed and pareto-scaled (mean-centered and divided by the square root of the standard deviation of each variable) to make features more comparable. Principal component analysis (PCA) was performed for outlier removal and data quality assessment. Significance analysis of microarray (SAM) was performed using the Siggenes R package.[38] SAM is a well-established statistical method for identification of differentially expressed genes in microarray data analysis and is frequently employed for analysis of high-throughput omics data sets.[39] It is designed to address the false discovery rate (FDR) when running multiple tests and high-dimensional data. SAM assigns a significance score to each

DOI: 10.1021/pr5009493
J. Proteome Res. 2015, 14, 411−421

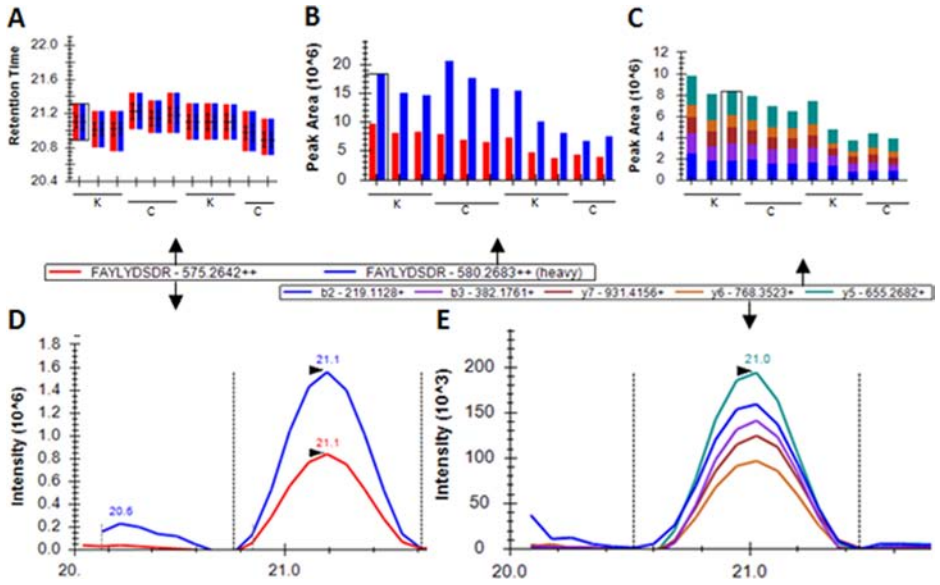

Figure 1. Representative retention time ranges (A), peak areas (B), and SRM mass spectrum (D) for the endogeneous (red, 576.264++) and isotopically labeled (blue, 580.2683++) peptide "FAYLYDSDR" of the glutamate receptor 2 (GRIA2_RAT) in a rat brain total lysate. Peak areas (C) and SRM mass spectrum (E) of the y ions of the endogenous "FAYLYDSDR" peptide. Samples were measured using triplicate injections. K = ketamine-treated rats, C = control.

variable on the basis of change relative to the standard deviation of repeated measurements. For a variable with scores greater than an adjustable threshold, its relative difference is compared with the distribution estimated by random permutation of the class labels. For each threshold, a certain proportion of the variables in the permutation set will be identified as significantly different by chance. This proportion is used to calculate the FDR. Analyses were conducted under blinded conditions with respect to sample identities, and samples were measured in random order to avoid any sequential biases, as described above.

BRAIN PROFILING

Sample Preparation

Frontal cortex and hippocampus tissue samples (10 ketamine-treated and 10 vehicle-treated rats for each region) were added to fractionation buffer containing 7 M urea, 2 M thiourea, 4% 3-[(3-cholamidopropyl)dimethylammonio]-1-propanesulfonate (CHAPS), 2% ASB14, 70 mM dithiotreitol (DTT), and protease inhibitors at a 5:1 (v/w) ratio.[40] Samples were sonicated (10 s, 2 cycles) and vortexed at 4 °C for 30 min. Samples were then centrifuged at 17 000*g* at 4 °C. Protein concentrations of the supernatants were determined in triplicate using a Bradford assay (Bio-Rad; Hemel Hempstead, U.K). Proteins (100 μg) were precipitated from each sample using acetone. After dissolving the precipitates in 100 μL of ammonium bicarbonate (50 mM) and protein concentration measurement, 40 μg of proteins was used for the reduction of the sulfhydryl groups with 5 mM DTT at 60 °C for 30 min, and alkylation was carried out using 10 mM iodacetamide via incubation in the dark at 37 °C for 30 min. Finally, the proteins were digested using trypsin at a 1:50 (w/v) ratio for 17 h at 37 °C, and the reactions were stopped by addition of 8.8 M HCl at a 1:60 (w/w) ratio.

Label-Based SRM Mass Spectrometry

The levels of 44 candidate proteins implicated in the molecular mechanisms of ketamine response or NMDAR function were measured in frontal cortical and hippocampal brain extracts (10 ketamine-treated and 10 vehicle-treated rats) using targeted SRM mass spectrometry on a Xevo TQ-S mass spectrometer (Waters Corporation; Milford, CT, USA) coupled online through a New Objective nanoESI emitter (7 cm length, 10 mm tip; New Objective) to a nanoAcquity UPLC system (Waters Corporation). The system consisted of a C18 trapping column (180 μm × 20 mm, 5 μm particle size) and a C18 BEH nanocolumn (75 μm × 200 mm, 1.7 mm particle size). The buffers used for separation were (A) 0.1% formic acid and (B) 0.1% formic acid in acetonitrile, and the following 48 min gradient was applied: 97/3% (A/B) to 60/40% in 30 min; 60/40% to 15/85% in 2 min; 5 min at 15/85%; returning to the initial condition in 1 min. The flow rate was 0.3 μL/min, and the column temperature was 35 °C.

Multiplex SRM assays were developed using a high-throughput strategy,[41] and the initial process assessed the suitability of over 200 selected proteins. Up to 12 unique peptides ranging from 6 to 20 amino acids in length, containing tryptic ends and no missed cleavages, were chosen for each of the selected proteins. All peptides containing amino acids prone to undergo modifications (e.g., Met, Trp, Asn, and Gln), potential ragged ends, or those with lysine/arginine followed by proline or bearing NXT/NXS glycosylation motifs were avoided and selected only when no other options were available.[42] Peptides were also checked by protein basic local alignment search tool (BLAST) (http://blast.ncbi.nlm.nih.gov/Blast.cgi) searches to ensure uniqueness. For method refinement, up to 12 transitions per peptide were tested in scheduled SRM mode using total rat brain lysates. Transitions were calculated using Skyline version 1.2.0.3425[43] and corresponded to singly charged y ions from doubly or triply charged precursors in the range of 350−1250 Da. Transitions were selected on the basis of software internal predictions, discovery proteomics data, and spectral data available through the Human NIST spectral libraries.[44]

For the final SRM assay, 1−3 peptides with at least 3 transitions of maximal intensity and highest spectral library

DOI: 10.1021/pr5009493
J. Proteome Res. 2015, 14, 411−421

similarity (dotp) were selected by manual inspection. Heavy labeled forms of the selected peptides (spiketides L) (2−3 peptides per protein) were chemically produced via SPOT synthesis (JPT Peptide Technologies GmBH, Berlin, Germany). We then analyzed heavy-label spiked rat brain lysate samples (Figure 1b) in scheduled SRM mode to confirm peptide identities via coelution, adjusted the amount of each heavy peptide to the endogenous counterpart, extracted the optimal fragment ions for SRM analysis, obtained accurate peptide retention times, and optimized collision energies and cone voltages for quantification runs using the Skyline software (MacCoss Lab Software; Seattle, WA, USA).[43] We intended to use at least two peptides from the same target proteins for increased accuracy; however, some peptides had to be excluded because of factors such as interference of matrix, nondetection, or mismatch of endogeneous and heavy labeled peptides. The final transitions, collision energies, and retention time windows used for each peptide can be found in the Supporting Information (Table 1a).

Quantitative SRM measurements comparing frontal cortical and hippocampal brain extracts from acute ketamine treated rats and controls were performed in scheduled SRM acquisition mode using the optimized parameters defined during assay refinement. For each target peptide, a heavy isotope labeled internal standard (JPT Peptide Technologies GmbH) was spiked in the peptide mixture for accurate quantification and identification. All SRM functions had a 2 min window of the predicted retention time, and scan times were 20 ms. For each peptide, at least three transitions were monitored for the heavy and light versions. Samples were run randomized and blocked[45] in triplicate, and blanks and quality control peptide injections (yeast alcohol dehydrogenase; Supporting Information Table 1b) were run alternating after each biological replicate. Resulting SRM data were analyzed using Skyline, and statistical analysis was conducted using SRMstats.[46] Data were manually inspected in Skyline, and problematic transitions (interference, low detection sensitivity, retention time shift) were deleted. A final list of transitions for relative quantification can be found in the Supporting Information (Table 1c).

Data preprocessing consisted of a $\log_2$ transformation to stabilize the variance. A constant normalization was performed on the basis of reference transitions to equalize the median peak intensities of reference transitions from all proteins across all MS runs and to adjust the bias to both reference and endogenous signals. As a second step, a median normalization of the median intensities of all transitions for each run was performed to correct for differences in protein loadings. PCA analysis was performed for outlier removal and further quality assessement. Protein level quantification and testing for differential abundance among acute ketamine- and vehicle-treated rats were carried out using the linear mixed-effects model implemented in SRMstats, which employs a "restricted" scope of conclusions.[47,48] In the restricted scope model, the individual samples being modeled were the population of interest. This approach also took into account the measurement error of transitions across runs (technical variation) to enable accurate quantification of protein abundance changes across the samples. The p values were adjusted to control for the false discovery rate at a cutoff of 0.05 according to Benjamini and Hochberg.[49]

RESULTS

Serum Profiling

Muliplex immunoassay profiling was carried out to determine ketamine-treatment-induced effects in blood serum. After data filtering, 66 analytes were measured in serum samples from ketamine-treated and control rats using a multiplex immunoassay platform (Supporting Information Table 2). Following data quality assessment, normalization and scaling, the analysis resulted in identification of three significantly changed analytes ($p^* < 0.05$) (Table 1). These were fibroblast growth factor 9 (FGF-9), interleukin (IL)-4 and tumor necrosis factor alpha (TNF-α).

Table 1. Significantly Changing Serum Analytes of the Acute Ketamine Rat Model (n = 9) Compared with Vehicle Treated Rats (n = 10) Identified by SAM[a]

analyte name	Uniprot KB number	ratio (K/C)[b]	P	P^*
fibroblast growth factor 9 (FGF-9)	P36364	0.65	8.23×10^{-05}	0.00345
IL-4 (interleukin-4)	P20093	0.91	0.00276	0.03852
tumor necrosis factor α (TNF-α)	P16599	0.86	0.00276	0.03852

[a] P^* = FDR-adjusted P; SAM = significance analysis of microarray, FDR = false discovery rate. [b] K = ketamine-treated rats; C = vehicle-treated rats.

Brain Tissue Profiling

We used SRM for targeted analysis to specifically investigate the effect of acute ketamine treatment on the abundance of key signaling proteins in rat frontal cortex and hippocampus. Tissues were chosen because the NMDAR is highly expressed in these regions,[50] and both regions have been implicated in the pathology of various psychiatric disorders, including schizophrenia[51] and MDD.[52,53] Therefore, we established a multiplex-SRM assay comprising proteins that have been implicated in the mechanism of action of NMDAR antagonists. This included signaling proteins involved in glutamatergic, GSK3β, mTOR, extracellular signal-regulated kinsase 1/2 (ERK1/2), and synaptic and energy functions as outlined in the introduction. An example assay for a peptide of the glutamate receptor 2 is shown in Figure 1. The analysis led to identification of 5 significantly changed proteins in the frontal cortex and 19 in the hippocampus of ketamine compared with vehicle-treated rats (see Table 2). Abnormalities in calcineurin and protein kinase Cβ (PKCβ) levels were detected in both brain regions. Intermediate filament proteins and the actin branching protein complex 2/3 were found to be altered in the frontal cortex, whereas mTOR, components of ERK signaling, PKCα, and synaptic vesicle endocytotic proteins [(vesicle fusing ATPase (NSF), synapsin (SYN1), syndapin-1 (PACN1)] were changed in the hippocampus (see Table 2). In addition, we detected an increase in the levels of mitochondrial aspartate aminotransferase (AATM) in the frontal cortex and hippocampus and a decrease in the levels of catechol-O-methyltransferase (COMT) in the hippocampus.

DISCUSSION

This is the first targeted proteomic study of serum and brain tissue from an acute ketamine rat model. Using a combination of sensitive proteomic platforms, we identified peripheral and

DOI: 10.1021/pr5009493
J. Proteome Res. 2015, 14, 411−421

Table 2. Significantly Changing Proteins Identified Using Label-Based LC−SRM Mass Spectrometry Profiling of the Acute Ketamine Rat Model[a] Compared with Vehicle Treated Rats[b,c]

							PCP rat models		KET rat	frontal cortex		hippocampus	
	uniprot entry name	protein name	gene name	biological function	TPP FC	TPP HC	chronic FC[66,99]	acute HC[35]	acute FC[65]	ratio (K/C)	*P**	ratio (K/C)	*P**
glutamate receptors	GRIA1	glutamate receptor 1	Gria1	ionotrophic glutamate receptor (AMPA1)	5|3	4|4				1.12	0.26	0.94	0.48
	GRIA2	glutamate receptor 2	Gria2	ionotrophic glutamate receptor (AMPA2)	4|5|3|5	5|4|5|5				1.09	0.39	0.99	0.95
	GRIA3	glutamate receptor 3	Gria3	ionotrophic glutamate receptor (AMPA3)	4|4	4|6				1.08	0.79	1.03	0.83
	NMDZ1	NMDA receptor 1	Grin1	NMDA receptor subtype, high calcium permeability	5	4				1.08	0.68	1.06	0.45
postsynaptic density	DLG4	disks large homologue 4	Dlg4	interacts with the NMDA receptor subunits	4|4	5|5				0.95	0.37	1.12	1.0×10^{-06}
	ACTN1	actinin-1	Actn1	F-actin cross-linking protein, interacts with PSD	2|1	4|4				1.04	0.79	0.77	1.6×10^{-07}
	ACTN2	actinin-2	Actn2	F-actin cross-linking protein	2|3	3|4				1.13	0.25	0.94	0.21
signal transduction	KCC2A	CamK2α	Camk2a	major protein kinase in the CNS, functions in LTP and neurotransmitter release	4|4	4	▼			0.96	0.79	0.94	0.32
	KCC2G	CamK2γ	Camk2g	function autonomously after Ca^{2+}/calmodulin-binding and autophosphorylation	4	5				0.94	0.25	1.14	0.0011
	PP2BB	calmodulin-dep. calcineurin A β	Ppp3cb	regulatory subunit of calcineurin, Ca^{2+}/calmodulin protein phosphatase	4|3	4|4	(▼)			1.14	0.036	0.90	0.041
	NCDN	neurochondrin	Ncdn	involved in signal transduction, increases cell surface localization of GRM5	4|4	4|5		▲		1.06	0.61	0.73	5.8×10^{-05}
	MK01	ERK2	Erk2	serine/threonine kinases, essential components of the MAPK signal transduction pathway	4|5|4	5|5|6				1.07	0.28	1.02	0.53
	MK03	ERK1	Erk1		4|4	5|4|3	▲			1.23	0.15*	0.90	0.041
	PEA15	PED	Pea15	blocks Ras-mediated inhibition of integrin activation, modulates ERK kinase cascade	8	8				1.04	0.78	0.66	$<10^{-15}$
	MTOR	mTOR	Mtor	central regulator of cellular metabolism, growth and survival	6|4	5|4				1.24	0.22	1.18	0.042
	CTNB1	catenin β-1	Ctnnb1	key downstream component of the canonical Wnt signaling pathway		3				not detected		1.20	0.11
	GSK3B	glycogen synthase kinase-3 β	Gsk3b	active protein kinase, neg. regulator in the hormonal control of glucose homeostasis	5|6	6|5				1.04	0.86	1.00	0.98
	KPCA	protein kinase C α type	Prkca	Ca^{2+}-act. Ser/Thr -protein kinases involved in cell proliferation, apoptosis, differentiation, migration	3|4|5	4|5				1.02	0.87	0.87	0.023
	KPCB	β type	Prkcb	involved in oxidative stress-induced apoptosis and insulin signaling	4	6				1.19	0.049	1.12	0.015
	KPCG	γ type	Prkcg	regulates neuronal receptor functions, mediates synaptic function	4|5|4|3	4|7|5|4				1.01	0.87	1.06	0.061
synaptic vesicle endo-/exocytosis	NSF	vesicle-fusing ATPase	Nsf	required for vesicle-mediated transport, influences GRIA2 membrane cycling	4|4|4	5|3|8				1.07	0.38	1.12	3.3×10^{-08}
	PACN1	syndapin-1	pacsin1	plays a role in neurite formation, required for synaptic vesicle endocytosis	4	5				0.99	0.95	1.12	0.023
	SYN1	synapsin-1	Syn-1	coats synaptic vesicles, binds cytoskeleton, regulation of neurotransmitter release	5|6	4|3	▲▲			0.98	0.88	0.85	0.0004
	SYNJ1	synaptojanin-1	Synj-1	interacts with ASH, GRB2	4|3	4|4	▼			0.87	0.049	1.05	0.26
	SYT1	synaptotagmin-1	Syt-1	trafficking of synaptic vesicles at the active zone	4|4	4|4				1.04	0.79	1.02	0.68

DOI: 10.1021/pr5009493
J. Proteome Res. 2015, 14, 411−421

Table 2. continued

	uniprot entry name	protein name	gene name	biological function	TPP FC	TPP HC	PCP rat models: chronic FC[66,99]	PCP rat models: acute HC[35]	KET rat: acute FC[65]	frontal cortex: ratio (K/C)	frontal cortex: *P**	hippocampus: ratio (K/C)	hippocampus: *P**
	VGLU1	vesicular glutamate transporter 1	Vglut	mediates uptake of glutamate into synaptic vesicles at excitatory neural cells	5	5	▲			1.04	0.79	1.06	0.12
neurotransmitter metabolism	AATM	aspartate aminotransferase, mitochondrial	Aatm	catalyzes a transaminase reaction producing L-glutamate	4|6	5|7				1.07	0.13*	1.06	0.041
	COMT	catechol *O*-methyltransferase	Comt	catalyzes *O*-methylation, thereby inactivation of catecholamine neurotransmitters		4				not detected		0.82	0.032
	DCE2	glutamate decarboxylase	Dce2	catalyzes the production of 4 amino-butanoate (GABA) from L-glutamate	4	4				0.98	0.87	1.06	0.32
	PROD	proline dehydrogenase 1, mitochondrial	Prod	catalyzes the degradation of L-proline		4				not detected		1.00	0.96
	GABT	GABA aminotransferase	Abat	catalyzes the conversion of GABA to two products	5|2	5				0.75	0.15*	1.02	0.69
energy	CMC1	mitochondrial asparate glutamate carrier 1	aralar1	catalyzes the calcium-dependent exchange of cytoplasmic glutamate and aspartate	3|3	5|7				0.72	0.87	1.16	0.19
	KPYM	pyruvate kinase, mitochondrial	Pkm	glycolytic enyzme, catalyzes phosphorylation of phosphoenolpyruvate	4|5	5|5				0.99	0.87	1.09	0.059
	NDUS1	complex I-75 kDa	Ndufs1	core subunit of mitochondrial respiratory chain NADH dehydrogenase	5|6	7|5	▲		▼	1.04	0.86	0.85	0.0045
cytoskeleton	intermediate filaments												
	GFAP	glial fibrillary acidic protein	Gfap	class II intermediate filament	4	5				1.12	0.38	0.69	3.9×10^{-14}
	AINX	α-internexin	Ina	class IV neuronal intermediate filament, involved in neuronal morphogenesis	6|6	7|6			▲	0.85	2.8×10^{-06}	0.99	0.53
	NFL	neurofilament light polypeptide	Nfl	neurofilament light polypeptide (NF-L)	5|4|6	5|5|5			▼	0.81	9.4×10^{-05}	1.14	0.0044
	actin cytoskeleton												
	COF1	cofilin-1	Cof1	exhibits F-actin depolymerizing activity, regulates actin cytoskeleton dynamics	5	5|3				1.02	0.61	1.02	0.79
	PROF1	profilin-1	Prof1	prevents the polymerization of actin	4|4	4|4				1.04	0.79	1.04	0.68
	ARPC2	Arp 2/3 complex 34 kDa subunit	Arpc2	regulation of actin polymerization, branched actin networks	5|7|5	4|5|6	(▼)	▼		1.15	0.064	1.08	0.19
	tubulin cytoskeleton												
	D3ZCE7	protein Tppp	Tppp	may play a role in the polymerization of tubulin in microtubules	6|5	5				0.99	0.87	1.04	0.26
oxidative stress	SODC	superoxide dismutase [Cu-Z]	Sod1	catalyzes the dismutation of superoxide into oxygen and hydrogen peroxide	4|4	4|5				1.02	0.86	1.03	0.50
	PARK7	protein DJ-1	Park7	protects cells against oxidative stress and cell death	4	4				0.93	0.26	1.02	0.67
	PHB	prohibitin	Phb	prohibitin inhibits DNA synthesis, role in regulating proliferation	4|4|4	4|5|4	▲	▼	▲	1.03	0.79	1.14	2.9×10^{-08}

[a] $n = 8$ for FC, $n = 10$ for HC. [b] $n = 9$ for FC, $n = 10$ for HC. [c] Findings were compared with those previously reported in frontal cortex and hippocampus of NMDAR antagonist rodent models (phencyclidine (PCP) and ketamine). *P* values were determined using SRMstats and corrected to control for multiple hypothesis testing[49] (*P** = FDR-adjusted *P*). Asterisks indicate proteins with significance values of $p < 0.05$. TPP = transitions per proteotypic peptide, KET or K = ketamine-treated rats, C = control rats, FC = frontal cortex, HC = hippocampus.

DOI: 10.1021/pr5009493
J. Proteome Res. 2015, 14, 411−421

central protein abundance changes, which are induced by acute ketamine treatment. Peripheral blood serum was analyzed as a potential source of biomarkers that could be used for monitoring brain effects of the ketamine treatment; however, multiplex immunoassay analysis identified ketamine-induced decreases in the serum levels of only three proteins (FGF-9, IL-4, and TNFα). This suggested that the acute effects of ketamine on peripheral systems were minor, and further studies targeting other physiological pathways are warranted to investigate this further. Nevertheless, the effects on the three proteins identified here are consistent with previous studies which reported anti-inflammatory properties of ketamine.[17] The findings are also in line with reports of ketamine-induced attenuations in the TNFα and cytokine response to an *Escherichia coli* endotoxin challenge[54] in rats and to an LPS insult in horses.[55] Nebulized ketamine treatment in actively sensitized brown Norway rats also led to decreased IL-4 levels.[56] In human studies, both ketamine and the NMDAR antagonist MK-801 have been shown to decrease TH cell differentiation along with IFN-γ and IL-4 production of peripheral blood mononuclear cells.[57] However, there are some inconsistencies of these findings with those from human schizophrenia studies. For example, higher serum levels of TNFα have been found in first-episode psychosis,[58] and a study that investigated a range of cytokines and hormones in serum reported that patients with an acute exacerbation of schizophrenia had increased TNFα and reduced IL-4 levels.[59]

The finding that ketamine induced changes in FGF-9 has not been reported previously. FGF-9 is mostly expressed in the adult and developing central nervous system and serves as a growth and survival factor for various cell types. It modulates the expression of myelin-related proteins and multiple fibroblast growth factor receptors in developing oligodendrocytes.[60] FGF9 also prevents the death of dopaminergic neurons and is involved in melatonin neuroprotection in vivo and in vitro.[61] Abnormal melatonin metabolism has been associated with schizophrenia since the early 1920s.[62] In addition, the effects of FGF-9 on glial fibrillary acidic protein (GFAP)-positive astrocytes have been shown,[63] suggesting a role for this growth factor in astrocyte differentiation. This is consistent with our finding of decreased GFAP levels in the hippocampus, demonstrating potential translation of effects on astrocyte function between the brain and periphery.

The main effects of the ketamine treatment in the brain involved changes in protein phosphatases and kinases. Interestingly, more of these changes were identified in the hippocampus, a brain region that is prominently involved in cognition and memory. The altered proteins included Ca^{2+}-calmodulin dependent protein kinases (CamK2), the mTOR and ERK kinases, and PKCβ. One study showed that acute PCP treatment, another NMDAR antagonist, induced extensive and distinct protein phosphorylation in the rat frontal cortex,[64] consistent with our findings. In the frontal cortex, we also substantiated the findings of previous studies that found abnormal levels of intermediate filaments (neurofilament light chain (NFL) and α-internexin)[65] and the actin-related protein complex 2/3.[66] These proteins are known to be involved in active synaptic development and remodeling[67] as well as in antidepressant treatment effects.[68,69]

As one of the most striking findings, we identified counter-regulated changes in the levels of calcineurin in the frontal cortex and hippocampus. This could be related to the well-established connection of these two brain regions through both excitatory glutamate neurons and inhibitory GABA receptor interneurons. Calcineurin is a neuron-enriched Ca^{2+}-calmodulin-dependent protein kinase that regulates synaptic plasticity. It has been associated with schizophrenia[70−72] and MDD,[73] and in the mechanism of action of antidepressants.[74] Conditional calcineurin knockout mice exhibit multiple abnormal behaviors related to schizophrenia,[72] and blockade of protein phosphatase 2B activity in the amygdala increases anxiety- and depression-like behaviors in mice.[75] Furthermore, chronic inhibition of calcineurin in the prefrontal cortex induces depression-like behavior through the mTOR pathway, which could be reversed by the antidepressant venlafaxine.[73] This is consistent with our finding of ketamine-induced increased calcineurin levels in the frontal cortex.

In line with the known effects of calcineurin in the mTOR pathway, we identified increased levels of the mTOR kinase. Activation of mTOR is essential for dendrite formation and regulation of spine growth,[76] which have been shown to be affected by acute ketamine treatment. Moreover, mTOR is also crucial for regulating the expression of several proteins involved in synaptic plasticity.[77] Reduced synaptic proteins in conjunction with reduced mTOR signaling have been reported in the prefrontal cortex of depressed patients.[78] Studies have shown that ketamine administration in rats induces a rapid induction of phosphorylation of mTOR, p70S6 kinase, and 4E-BP1[79] in PFC synaptoneurosome preparations, accompanied by an upregulation of synaptic plasticity markers such as postsynaptic density protein 95 (PSD95). We found that PSD95 is increased in the hippocampus. Recent studies have suggested that ketamine produces antidepressant actions via stimulation of mTOR, and this leads to increased levels of synaptic proteins in the prefrontal cortex. Therefore, the current findings support the targeting of the mTOR signaling pathway as a promising approach in the development of new antidepressant or antipsychotic drugs.

Our findings of decreased neurochondrin in the hippocampus are interesting because this protein has recently been shown to modulate the activity of the metabolic glutamate receptor 5 (mGluR5), which has been implicated in several neuropsychiatric disorders, including schizophrenia.[80,81] Conditional knockout of neurochondrin in transgenic mice reduces mGluR5 function and associated defects in prepulse inhibition and psychostimulant-induced locomotor activity, two behavioral phenotypes typically observed in rodent models of schizophrenia. In the case of MDD, the preclinical and clinical data indicates that mGluR5-antagonists also have antidepressant-like and anxiolytic-like drug effects, but they also have the same problem of psychotomimetic activity as found for NMDA-receptor antagonists in the treatment of depression.[82] We also found increased levels of PKCβ in the frontal cortex and the hippocampus. PKC is involved in the phosphorylation of many proteins and may consequently cause widespread alterations in many physiological processes. For instance, PKC overactivity impairs prefrontal cortical regulation of working memory, which has been identified as a core dysfunction in schizophrenia.[83] In addition, PKC abnormalities have been implicated in schizophrenia pathology and response to psychotropic medications.[84] It should also be noted that PKCβ regulates dopamine D_2 autoreceptor activated transporter trafficking and dopaminergic signaling, which regulates the strength and duration of extracellular dopamine concentrations.[85] Hence, PKCβ may represent a potential drug target for correcting abnormal extracellular dopamine levels in

DOI: 10.1021/pr5009493
J. Proteome Res. 2015, 14, 411−421

diseases such as schizophrenia and MDD. Combined SSRI and antipsychotic treatment has already been associated with changes in PKCβ in patients.[86]

Investigating alterations of key enzymes of neurotransmitter metabolism, the current study found decreased levels of COMT in the hippocampus. This enzyme modulates dopamine, norepinephrine, and epinephrine levels. COMT has also been implicated by systematic[87] and candidate gene approaches[88,89] as a risk gene for schizophrenia. It also has been shown to play a role in symptom severity in MDD.[90] Consistent with our findings, another study found that the dopamine modulating enzymes 3,4-dihydroxyphenylacetic acid and homovanillic acid were increased specifically in the hippocampus after acute ketamine treatment.[16] We also detected an increase in AATM in the frontal cortex and hippocampus. Decreased levels of AATM in the frontal cortex have been shown in a chronic PCP rat model for schizophrenia[66] and alterations in glutamate metabolism in preclinical[91,92] and clinical studies of schizophrenia[93,94] and depression.[95] A recent comprehensive proteomic study found changes that supported a glutamatergic hypofunction in schizophrenia prefrontal cortex and hyperfunction in MDD.[97]

This study also found changes in the levels of proteins involved in endo- and exocytosis. These pathways are a component of the synaptic vesicle cycling, crucial for presynaptic and postsynaptic functions, such as release and reuptake of neurotransmitters. Consistent with this, we also found novel changes in proteins in the hippocampus that may be relevant in the context of schizophrenia and depression. These included a decrease in the levels of SYN1 and an increase in vesicle fusing ATPase (NSF), which is specifically involved in AMPA receptor trafficking. Effects on both endo- and exocytosis have been previously linked to schizophrenia[96] as well as to PCP-induced psychosis in a rat model.[66,98]

CONCLUSIONS

The study validates known features and identifies several novel molecular aspects of acute ketamine treatment. Testing a wide range of previously described hypotheses, this is the first and largest targeted study to decipher the effects of ketamine at the protein level in the brain and periphery. The brain analyses provided molecular correlates of ketamine effects, which may be useful as biomarkers for development of novel drugs in the treatment of schizophrenia and depressive disorders. This demonstrated the utility of SRM mass spectrometry for analysis of changes in the levels of proteins comprising key networks involved in these disorders or in the mechanism of action of the associated medications. Specifically, this analysis led to identification of ketamine-induced effects on signaling pathways involved in synaptic plasticity. Predominately, the levels of kinases and phosphatases were altered, and the hippocampus was affected more strongly than the frontal cortex. The established targeted screen using the SRM mass spectrometry of brain proteins will help to accelerate preclinical validation toward clinical translation and offers a feasible pipeline for candidate drug target identification and drug development. Serum profiling analysis using the targeted multiplex immunoassay platform resulted in identification of only three proteins altered by acute ketamine treatment. These were associated with inflammation and growth factor signaling. Further studies using assays targeting additional pathways could lead to identification of peripheral biomarkers for use in clinical studies. The study increases the clinical validity of the ketamine model and, through its focus on protein phosphatases and kinases in the brain, which represent drug targets.

ASSOCIATED CONTENT

Supporting Information

(Table S1a–c) Full information for all transitions in the multiplexed SRM-assay: (a) Measured transitions, (b) alcohol dehydrogenase quality control injections, and (c) filtered transitions for relative quantification. (Table S2) Full information for all measurable analytes using multiplexed immunoassay profiling. This material is available free of charge via the Internet at http://pubs.acs.org.

AUTHOR INFORMATION

Corresponding Author

*Phone: +44 (0) 1223334151. E-mail: sb209@cam.ac.uk.

Notes

The authors declare the following competing financial interest(s): S.B. is a consultant for Myriad-RBM. This does not affect policies regarding sharing of data and materials specified by this journal. None of the other authors declare a conflict of interest.

ACKNOWLEDGMENTS

This research was kindly supported by the Stanley Medical Research Institute (SMRI), the Innovative Medicines Initiative for Novel Methods leading to New Medications in Depression and Schizophrenia (IMI NEWMEDS) and the Dutch Fund for Economic Structure Reinforcement ((No. 0908) the Neuro-Basic PharmaPhenomics project.

REFERENCES

(1) Zarate, C. A., Jr.; Singh, J. B.; Carlson, P. J.; Brutsche, N. E.; Ameli, R.; Luckenbaugh, D. A.; Charney, D. S.; Manji, H. K. A randomized trial of an *N*-methyl-D-aspartate antagonist in treatment-resistant major depression. *Arch. Gen. Psychiatry* **2006**, *63* (8), 856–864.

(2) Zarate, C. A., Jr.; Singh, J. B.; Quiroz, J. A.; De Jesus, G.; Denicoff, K. K.; Luckenbaugh, D. A.; Manji, H. K.; Charney, D. S. A double-blind, placebo-controlled study of memantine in the treatment of major depression. *Am. J. Psychiatry* **2006**, *163* (1), 153–155.

(3) Kapur, S.; Seeman, P. NMDA receptor antagonists ketamine and PCP have direct effects on the dopamine D(2) and serotonin 5-HT(2) receptors-implications for models of schizophrenia. *Mol. Psychiatry* **2002**, *7* (8), 837–844.

(4) Horiguchi, M.; Hannaway, K. E.; Adelekun, A. E.; Huang, M.; Jayathilake, K.; Meltzer, H. Y. D-1 receptor agonists reverse the subchronic phencyclidine (PCP)-induced novel object recognition (NOR) deficit in female rats. *Behav. Brain Res.* **2013**, *238*, 36–43.

(5) Becker, A.; Peters, B.; Schroeder, H.; Mann, T.; Huether, G.; Grecksch, G. Ketamine-induced changes in rat behaviour: A possible animal model of schizophrenia. *Prog. Neuropsychopharmacol. Biol. Psychiatry* **2003**, *27* (4), 687–700.

(6) Gastambide, F.; Mitchell, S. N.; Robbins, T. W.; Tricklebank, M. D.; Gilmour, G. Temporally distinct cognitive effects following acute administration of ketamine and phencyclidine in the rat. *Eur. Neuropsychopharmacol.* **2013**, *23* (11), 1414–1422.

(7) Lipska, B. K.; Weinberger, D. R. To model a psychiatric disorder in animals: schizophrenia as a reality test. *Neuropsychopharmacology* **2000**, *23* (3), 223–239.

(8) Bubenikova-Valesova, V.; Horacek, J.; Vrajova, M.; Hoschl, C. Models of schizophrenia in humans and animals based on inhibition of NMDA receptors. *Neurosci. Biobehav. Rev.* **2008**, *32* (5), 1014–1023.

DOI: 10.1021/pr5009493
J. Proteome Res. 2015, 14, 411–421

(9) Zugno, A. I.; de Miranda, I. M.; Budni, J.; Volpato, A. M.; Luca, R. D.; Deroza, P. F.; de Oliveira, M. B.; Heylmann, A. S.; Silveira, F. D.; Wessler, P.; Mastella, G. A.; Cipriano, A. L.; Quevedo, J. Effect of maternal deprivation on acetylcholinesterase activity and behavioral changes on the ketamine-induced animal model of schizophrenia. *Neuroscience* **2013**, *248*, 252−260.
(10) Li, N. X.; Lee, B.; Liu, R. J.; Banasr, M.; Dwyer, J. M.; Iwata, M.; Li, X. Y.; Aghajanian, G.; Duman, R. S. mTOR-Dependent synapse formation underlies the rapid antidepressant effects of NMDA antagonists. *Science* **2010**, *329* (5994), 959−964.
(11) Garcia, L. S.; Comim, C. M.; Valvassori, S. S.; Reus, G. Z.; Barbosa, L. M.; Andreazza, A. C.; Stertz, L.; Fries, G. R.; Gavioli, E. C.; Kapczinski, F.; Quevedo, J. Acute administration of ketamine induces antidepressant-like effects in the forced swimming test and increases BDNF levels in the rat hippocampus. *Prog. Neuropsychopharmacol. Biol. Psychiatry* **2008**, *32* (1), 140−144.
(12) Koike, H.; Iijima, M.; Chaki, S. Involvement of AMPA receptor in both the rapid and sustained antidepressant-like effects of ketamine in animal models of depression. *Behav. Brain Res.* **2011**, *224* (1), 107−111.
(13) Garcia, L. S.; Comim, C. M.; Valvassori, S. S.; Reus, G. Z.; Stertz, L.; Kapczinski, F.; Gavioli, E. C.; Quevedo, J. Ketamine treatment reverses behavioral and physiological alterations induced by chronic mild stress in rats. *Prog. Neuropsychopharmacol. Biol. Psychiatry* **2009**, *33* (3), 450−455.
(14) Autry, A. E.; Adachi, M.; Nosyreva, E.; Na, E. S.; Los, M. F.; Cheng, P. F.; Kavalali, E. T.; Monteggia, L. M. NMDA receptor blockade at rest triggers rapid behavioural antidepressant responses. *Nature* **2011**, *475* (7354), 91−U109.
(15) Li, N. X.; Liu, R. J.; Dwyer, J. M.; Banasr, M.; Lee, B.; Son, H.; Li, X. Y.; Aghajanian, G.; Duman, R. S. Glutamate *N*-methyl-D-aspartate receptor antagonists rapidly reverse behavioral and synaptic deficits caused by chronic stress exposure. *Biol. Psychiatry* **2011**, *69* (8), 754−761.
(16) Chatterjee, M.; Verma, R.; Ganguly, S.; Palit, G. Neurochemical and molecular characterization of ketamine-induced experimental psychosis model in mice. *Neuropharmacology* **2012**, *63* (6), 1161−1171.
(17) De Kock, M.; Loix, S.; Lavand'homme, P. Ketamine and peripheral inflammation. *CNS Neurosci. Ther.* **2013**, *19* (6), 403−410.
(18) Hurley, L. L.; Tizabi, Y. Neuroinflammation, neurodegeneration, and depression. *Neurotoxic. Res.* **2013**, *23* (2), 131−144.
(19) Park, S. W.; Lee, J. G.; Seo, M. K.; Lee, C. H.; Cho, H. Y.; Lee, B. J.; Seol, W.; Kim, Y. H. Differential effects of antidepressant drugs on mTOR signalling in rat hippocampal neurons. *Int. J. Neuropsychopharmacol.* **2014**, *17*, 1−16.
(20) Huang, L.; Liu, Y.; Jin, W.; Ji, X.; Dong, Z. Ketamine potentiates hippocampal neurodegeneration and persistent learning and memory impairment through the PKCgamma-ERK signaling pathway in the developing brain. *Brain Res.* **2012**, *1476*, 164−171.
(21) Reus, G. Z.; Vieira, F. G.; Abelaira, H. M.; Michels, M.; Tomaz, D. B.; Dos Santos, M. A.; Carlessi, A. S.; Neotti, M. V.; Matias, B. I.; Luz, J. R.; Dal-Pizzol, F.; Quevedo, J. MAPK signaling correlates with the antidepressant effects of ketamine. *J. Psychiatr. Res.* **2014**, *55*, 15−21.
(22) Kavalaii, E. T.; Monteggia, L. M. Synaptic mechanisms underlying rapid antidepressant action of ketamine. *Am. J. Psychiatry* **2012**, *169* (11), 1150−1156.
(23) Naughton, M.; Clarke, G.; O'Leary, O. F.; Cryan, J. F.; Dinan, T. G. A review of ketamine in affective disorders: Current evidence of clinical efficacy, limitations of use and pre-clinical evidence on proposed mechanisms of action. *J. Affective Disord.* **2014**, *156*, 24−35.
(24) Rosso, S. B.; Sussman, D.; Wynshaw-Boris, A.; Salinas, P. C. WNT signaling through dishevelled, Rac and JNK regulates dendritic development. *Nat. Neurosci.* **2005**, *8* (1), 34−42.
(25) Bai, X. W.; Yan, Y. S.; Canfield, S.; Muravyeva, M. Y.; Kikuchi, C.; Zaja, I.; Corbett, J. A.; Bosnjak, Z. J. Ketamine enhances human neural stem cell proliferation and induces neuronal apoptosis via reactive oxygen species-mediated mitochondrial pathway. *Anesth. Analg.* **2013**, *116* (4), 869−880.
(26) de Oliveira, L.; Spiazzi, C. M. D.; Bortolin, T.; Canever, L.; Petronilho, F.; Mina, F. G.; Dal-Pizzol, F.; Quevedo, J.; Zugno, A. I. Different sub-anesthetic doses of ketamine increase oxidative stress in the brain of rats. *Prog. Neuro-Psychopharmacol. Biol. Psychiatry* **2009**, *33* (6), 1003−1008.
(27) Zugno, A. I.; Chipindo, H. L.; Volpato, A. M.; Budni, J.; Steckert, A. V.; de Oliveira, M. B.; Heylmann, A. S.; Silveira, F. D.; Mastella, G. A.; Maravai, S. G.; Wessler, P. G.; Binatti, A. R.; Panizzutti, B.; Schuck, P. F.; Quevedo, J.; Gama, C. S. Omega-3 prevents behavior response and brain oxidative damage in the ketamine model of schizophrenia. *Neuroscience* **2014**, *259*, 223−231.
(28) Rezin, G. T.; Goncalves, C. L.; Daufenbach, J. F.; Fraga, D. B.; Santos, P. M.; Ferreira, G. K.; Hermani, F. V.; Comim, C. M.; Quevedo, J.; Streck, E. L. Acute administration of ketamine reverses the inhibition of mitochondrial respiratory chain induced by chronic mild stress. *Brain Res. Bull.* **2009**, *79* (6), 418−421.
(29) Hroudova, J.; Fisar, Z. In vitro inhibition of mitochondrial respiratory rate by antidepressants. *Toxicol. Lett.* **2012**, *213* (3), 345−352.
(30) Littlewood, C. L.; Jones, N.; O'Neill, M. J.; Mitchell, S. N.; Tricklebank, M.; Williams, S. C. Mapping the central effects of ketamine in the rat using pharmacological MRI. *Psychopharmacology (Berlin)* **2006**, *186* (1), 64−81.
(31) Li, J.; Ishiwari, K.; Conway, M. W.; Francois, J.; Huxter, J.; Lowry, J. P.; Schwarz, A. J.; Tricklebank, M.; Gilmour, G. Dissociable effects of antipsychotics on ketamine-induced changes in regional oxygenation and inter-regional coherence of low frequency oxygen fluctuations in the rat. *Neuropsychopharmacology* **2014**, *39* (7), 1635−1644.
(32) Gastambide, F.; Mitchell, S. N.; Robbins, T. W.; Tricklebank, M. D.; Gilmour, G. Temporally distinct cognitive effects following acute administration of ketamine and phencyclidine in the rat. *Eur. Neuropsychopharmacol.* **2013**, *23* (11), 1414−1422.
(33) Smith, J. W.; Gastambide, F.; Gilmour, G.; Dix, S.; Foss, J.; Lloyd, K.; Malik, N.; Tricklebank, M. A comparison of the effects of ketamine and phencyclidine with other antagonists of the NMDA receptor in rodent assays of attention and working memory. *Psychopharmacology* **2011**, *217* (2), 255−269.
(34) Paxinos, G.; Watson, C. *The Rat Brain in Stereotaxic Coordinates*, 4th ed.; Academic Press: San Diego, 1998; p 1v.
(35) Ernst, A.; Ma, D.; Garcia-Perez, I.; Tsang, T. M.; Kluge, W.; Schwarz, E.; Guest, P. C.; Holmes, E.; Sarnyai, Z.; Bahn, S. Molecular validation of the acute phencyclidine rat model for schizophrenia: identification of translational changes in energy metabolism and neurotransmission. *J. Proteome Res.* **2012**, *11* (7), 3704−3714.
(36) Ernst, A.; Sharma, A. N.; Elased, K. M.; Guest, P. C.; Rahmoune, H.; Bahn, S. Diabetic db/db mice exhibit central nervous system and peripheral molecular alterations as seen in neurological disorders. *Translational Psychiatry* **2013**, 3.
(37) Hackstadt, A. J.; Hess, A. M. Filtering for increased power for microarray data analysis. *BMC Bioinf.* **2009**, *10*, 11.
(38) Schwender, H., Siggenes: Multiple testing using SAM and Efron's empirical Bayes approaches. *R Package*, version 1.38.0; 2012.
(39) Tusher, V. G.; Tibshirani, R.; Chu, G. Significance analysis of microarrays applied to the ionizing radiation response. *Proc. Natl. Acad. Sci. U.S.A.* **2001**, *98* (9), 5116−5121.
(40) Martins-de-Souza, D.; Menezes de Oliveira, B.; dos Santos Farias, A.; Horiuchi, R. S.; Crepaldi Domingues, C.; de Paula, E.; Marangoni, S.; Gattaz, W. F.; Dias-Neto, E.; Camillo Novello, J. The use of ASB-14 in combination with CHAPS is the best for solubilization of human brain proteins for two-dimensional gel electrophoresis. *Briefings Funct. Genomic Proteomics* **2007**, *6* (1), 70−75.
(41) Picotti, P.; Rinner, O.; Stallmach, R.; Dautel, F.; Farrah, T.; Domon, B.; Wenschuh, H.; Aebersold, R. High-throughput generation of selected reaction-monitoring assays for proteins and proteomes. *Nat. Methods* **2010**, *7* (1), 43−U5.

DOI: 10.1021/pr5009493
J. Proteome Res. 2015, 14, 411−421

(42) Lange, V.; Malmstrom, J. A.; Didion, J.; King, N. L.; Johansson, B. P.; Schafer, J.; Rameseder, J.; Wong, C. H.; Deutsch, E. W.; Brusniak, M. Y.; Buhlmann, P.; Bjorck, L.; Domon, B.; Aebersold, R. Targeted quantitative analysis of *Streptococcus pyogenes* virulence factors by multiple reaction monitoring. *Mol. Cell. Proteomics* **2008**, *7* (8), 1489−1500.
(43) MacLean, B.; Tomazela, D. M.; Shulman, N.; Chambers, M.; Finney, G. L.; Frewen, B.; Kern, R.; Tabb, D. L.; Liebler, D. C.; MacCoss, M. J. Skyline: an open source document editor for creating and analyzing targeted proteomics experiments. *Bioinformatics* **2010**, *26* (7), 966−968.
(44) Farrah, T.; Deutsch, E. W.; Omenn, G. S.; Campbell, D. S.; Sun, Z.; Bletz, J. A.; Mallick, P.; Katz, J. E.; Malmstrom, J.; Ossola, R.; Watts, J. D.; Lin, B. A. Y.; Zhang, H.; Moritz, R. L.; Aebersold, R. A high-confidence human plasma proteome reference set with estimated concentrations in peptide atlas. *Mol. Cell. Proteomics* **2011**, *10*, (9).
(45) Oberg, A. L.; Vitek, O. Statistical design of quantitative mass spectrometry-based proteomic experiments. *J. Proteome Res.* **2009**, *8* (5), 2144−56.
(46) Chang, C. Y.; Picotti, P.; Huttenhain, R.; Heinzelmann-Schwarz, V.; Jovanovic, M.; Aebersold, R.; Vitek, O. Protein significance analysis in selected reaction monitoring (SRM) measurements. *Mol. Cell. Proteomics* **2012**, *11*, (4), 10.1074/mcp.M111.014662.
(47) Jin, L. L.; Tong, J. F.; Prakash, A.; Peterman, S. M.; St-Germain, J. R.; Taylor, P.; Trudel, S.; Moran, M. F. Measurement of protein phosphorylation stoichiometry by selected reaction monitoring mass spectrometry. *J. Proteome Res.* **2010**, *9* (5), 2752−2761.
(48) Surinova, S.; Huttenhain, R.; Chang, C. Y.; Espona, L.; Vitek, O.; Aebersold, R. Automated selected reaction monitoring data analysis workflow for large-scale targeted proteomic studies. *Nat. Protoc.* **2013**, *8* (8), 1602−1619.
(49) Benjamini, Y.; Hochberg, Y. Controlling the false discovery rate - a practical and powerful approach to multiple testing. *J. R. Stat. Soc., Series B, Methodol.* **1995**, *57* (1), 289−300.
(50) Ramsey, A. J. NR1 knockdown mice as a representative model of the glutamate hypothesis of schizophrenia. *Prog. Brain Res.* **2009**, *179*, 51−58.
(51) Tandon, R.; Keshavan, M. S.; Nasrallah, H. A. Schizophrenia, "just the facts" what we know in 2008. 2. Epidemiology and etiology. *Schizophr. Res.* **2008**, *102* (1−3), 1−18.
(52) Treadway, M. T.; Waskom, M. L.; Dillon, D. G.; Holmes, A. J.; Park, M. T.; Chakravarty, M. M.; Dutra, S. J.; Polli, F. E.; Iosifescu, D. V.; Fava, M.; Gabrieli, J. D.; Pizzagalli, D. A. Illness progression, recent stress, and morphometry of hippocampal subfields and medial prefrontal cortex in major depression. *Biol. Psychiatry* **2014**, 10.1016/j.biopsych.2014.06.018.
(53) Campbell, S.; Macqueen, G. The role of the hippocampus in the pathophysiology of major depression. *J. Psychiatry Neurosci.* **2004**, *29* (6), 417−426.
(54) Taniguchi, T.; Kanakura, H.; Takemoto, Y.; Kidani, Y.; Yamamoto, K. Effects of ketamine and propofol on the ratio of interleukin-6 to interleukin-10 during endotoxemia in rats. *Tohoku J. Exp. Med.* **2003**, *200* (2), 85−92.
(55) Lankveld, D. P.; Bull, S.; Van Dijk, P.; Fink-Gremmels, J.; Hellebrekers, L. J. Ketamine inhibits LPS-induced tumour necrosis factor-α and interleukin-6 in an equine macrophage cell line. *Vet. Res.* **2005**, *36* (2), 257−262.
(56) Zhu, M. M.; Zhou, Q. H.; Zhu, M. H.; Rong, H. B.; Xu, Y. M.; Qian, Y. N.; Fu, C. Z. Effects of nebulized ketamine on allergen-induced airway hyperresponsiveness and inflammation in actively sensitized Brown-Norway rats. *J. Inflamm. (London)* **2007**, *4*, 10.
(57) Gao, M.; Jin, W. J.; Qian, Y. N.; Ji, L. L.; Feng, G. B.; Sun, J. Effect of *N*-methyl-D-aspartate receptor antagonist on T helper cell differentiation induced by phorbol−myristate−acetate and ionomycin. *Cytokine* **2011**, *56* (2), 458−465.
(58) Di Nicola, M.; Cattaneo, A.; Hepgul, N.; Di Forti, M.; Aitchison, K. J.; Janiri, L.; Murray, R. M.; Dazzan, P.; Pariante, C. M.; Mondelli, V. Serum and gene expression profile of cytokines in first-episode psychosis. *Brain, Behav., Immun.* **2013**, *31*, 90−95.
(59) O'Brien, S. M.; Scully, P.; Dinan, T. G. Increased tumor necrosis factor-α concentrations with interleukin-4 concentrations in exacerbations of schizophrenia. *Psychiatry Res.* **2008**, *160* (3), 256−62.
(60) Cohen, R. I.; Chandross, K. J. Fibroblast growth factor-9 modulates the expression of myelin related proteins and multiple fibroblast growth factor receptors in developing oligodendrocytes. *J. Neurosci. Res.* **2000**, *61* (3), 273−287.
(61) Huang, J. Y.; Hong, Y. T.; Chuang, J. I. Fibroblast growth factor 9 prevents MPP+-induced death of dopaminergic neurons and is involved in melatonin neuroprotection in vivo and in vitro. *J. Neurochem.* **2009**, *109* (5), 1400−1412.
(62) Morera-Fumero, A. L.; Abreu-Gonzalez, P. Role of melatonin in schizophrenia. *Int. J. Mol. Sci.* **2013**, *14* (5), 9037−9050.
(63) Nakamura, S.; Todo, T.; Motoi, Y.; Haga, S.; Aizawa, T.; Ueki, A.; Ikeda, K. Glial expression of fibroblast growth factor-9 in rat central nervous system. *Glia* **1999**, *28* (1), 53−65.
(64) Palmowski, P.; Rogowska-Wrzesinska, A.; Williamson, J.; Beck, H. C.; Mikkelsen, J. D.; Hansen, H. H.; Jensen, O. N. Acute phencyclidine treatment induces extensive and distinct protein phosphorylation in rat frontal cortex. *J. Proteome Res.* **2014**, *13* (3), 1578−1592.
(65) Smalla, K. H.; Mikhaylova, M.; Sahin, J.; Bernstein, H. G.; Bogerts, B.; Schmitt, A.; van der Schors, R.; Smit, A. B.; Li, K. W.; Gundelfinger, E. D.; Kreutz, M. R. A comparison of the synaptic proteome in human chronic schizophrenia and rat ketamine psychosis suggests that prohibitin is involved in the synaptic pathology of schizophrenia. *Mol. Psychiatry* **2008**, *13* (9), 878−896.
(66) Wesseling, H.; Chan, M. K.; Tsang, T. M.; Ernst, A.; Peters, F.; Guest, P. C.; Holmes, E.; Bahn, S. A combined metabonomic and proteomic approach identifies frontal cortex changes in a chronic phencyclidine rat model in relation to human schizophrenia brain pathology. *Neuropsychopharmacology* **2013**, *38* (12), 2532−2544.
(67) Kim, I. H.; Racz, B.; Wang, H.; Burianek, L.; Weinberg, R.; Yasuda, R.; Wetsel, W. C.; Soderling, S. H. Disruption of Arp2/3 results in asymmetric structural plasticity of dendritic spines and progressive synaptic and behavioral abnormalities. *J. Neurosci.* **2013**, *33* (14), 6081−6092.
(68) Guest, P. C.; Knowles, M. R.; Molon-Noblot, S.; Salim, K.; Smith, D.; Murray, F.; Laroque, P.; Hunt, S. P.; De Felipe, C.; Rupniak, N. M.; McAllister, G. Mechanisms of action of the antidepressants fluoxetine and the substance P antagonist L-000760735 are associated with altered neurofilaments and synaptic remodeling. *Brain Res.* **2004**, *1002* (1−2), 1−10.
(69) Reines, A.; Cereseto, M.; Ferrero, A.; Sifonios, L.; Podesta, M. F.; Wikinski, S. Maintenance treatment with fluoxetine is necessary to sustain normal levels of synaptic markers in an experimental model of depression: correlation with behavioral response. *Neuropsychopharmacology* **2008**, *33* (8), 1896−1908.
(70) Gerber, D. J.; Hall, D.; Miyakawa, T.; Demars, S.; Gogos, J. A.; Karayiorgou, M.; Tonegawa, S. Evidence for association of schizophrenia with genetic variation in the 8p21.3 gene, PPP3CC, encoding the calcineurin gamma subunit. *Proc. Natl. Acad. Sci. U.S.A.* **2003**, *100* (15), 8993−8998.
(71) Eastwood, S. L.; Burnet, P. W.; Harrison, P. J. Decreased hippocampal expression of the susceptibility gene PPP3CC and other calcineurin subunits in schizophrenia. *Biol. Psychiatry* **2005**, *57* (7), 702−710.
(72) Miyakawa, T.; Leiter, L. M.; Gerber, D. J.; Gainetdinov, R. R.; Sotnikova, T. D.; Zeng, H.; Caron, M. G.; Tonegawa, S. Conditional calcineurin knockout mice exhibit multiple abnormal behaviors related to schizophrenia. *Proc. Natl. Acad. Sci. U.S.A.* **2003**, *100* (15), 8987−3992.
(73) Yu, J. J.; Zhang, Y.; Wang, Y.; Wen, Z. Y.; Liu, X. H.; Qin, J.; Yang, J. L. Inhibition of calcineurin in the prefrontal cortex induced depressive-like behavior through mTOR signaling pathway. *Psychopharmacology* **2013**, *225* (2), 361−372.
(74) Crozatier, C.; Farley, S.; Mansuy, I. M.; Dumas, S.; Giros, B.; Tzavara, E. T. Calcineurin (protein phosphatase 2B) is involved in the

DOI: 10.1021/pr5009493
J. Proteome Res. 2015, 14, 411−421

mechanisms of action of antidepressants. *Neuroscience* **2007**, *144* (4), 1470−1476.
(75) Bahi, A.; Mineur, Y. S.; Picciotto, M. R. Blockade of protein phosphatase 2B activity in the amygdala increases anxiety- and depression-like behaviors in mice. *Biol. Psychiatry* **2009**, *66* (12), 1139−1146.
(76) Li, L. A.; Xu, B. Z.; Zhu, Y.; Chen, L.; Sokabe, M.; Chen, L. DHEA prevents A beta(25−35)-impaired survival of newborn neurons in the dentate gyrus through a modulation of PI3K-Akt-mTOR signaling. *Neuropharmacology* **2010**, *59* (4−5), 323−333.
(77) Dwyer, J. M.; Duman, R. S. Activation of mammalian target of rapamycin and synaptogenesis: role in the actions of rapid-acting antidepressants. *Biol. Psychiatry* **2013**, *73* (12), 1189−1198.
(78) Jernigan, C. S.; Goswami, D. B.; Austin, M. C.; Iyo, A. H.; Chandran, A.; Stockmeier, C. A.; Karolewicz, B. The mTOR signaling pathway in the prefrontal cortex is compromised in major depressive disorder. *Prog. Neuro-Psychopharmacol. Biol. Psychiatry* **2011**, *35* (7), 1774−1779.
(79) Hoeffer, C. A.; Klann, E. mTOR signaling: At the crossroads of plasticity, memory and disease. *Trends Neurosci.* **2010**, *33* (2), 67−75.
(80) Bear, M. F.; Huber, K. M.; Warren, S. T. The mGluR theory of fragile X mental retardation. *Trends Neurosci.* **2004**, *27* (7), 370−377.
(81) Nakanishi, S.; Nakajima, Y.; Masu, M.; Ueda, Y.; Nakahara, K.; Watanabe, D.; Yamaguchi, S.; Kawabata, S.; Okada, M. Glutamate receptors: brain function and signal transduction. *Brain Res. Brain Res. Rev.* **1998**, *26* (2−3), 230−235.
(82) Palucha, A.; Pilc, A. Metabotropic glutamate receptor ligands as possible anxiolytic and antidepressant drugs. *Pharmacol. Ther.* **2007**, *115* (1), 116−147.
(83) Silver, H.; Feldman, P.; Bilker, W.; Gur, R. C. Working memory deficit as a core neuropsychological dysfunction in schizophrenia. *Am. J. Psychiatry* **2003**, *160* (10), 1809−1816.
(84) Arnsten, A. F. Ameliorating prefrontal cortical dysfunction in mental illness: inhibition of phosphotidyl inositol-protein kinase C signaling. *Psychopharmacology (Berlin)* **2009**, *202* (1−3), 445−455.
(85) Chen, R.; Daining, C. P.; Sun, H.; Fraser, R.; Stokes, S. L.; Leitges, M.; Gnegy, M. E. Protein kinase C is a modulator of the dopamine D2 autoreceptor-activated trafficking of the dopamine transporter. *J. Neurochem.* **2013**, *125* (5), 663−672.
(86) Silver, H.; Susser, E.; Danovich, L.; Bilker, W.; Youdim, M.; Goldin, V.; Weinreb, O. SSRI augmentation of antipsychotic alters expression of GABA(A) receptor and related genes in PMC of schizophrenia patients. *Int. J. Neuropsychopharmacol.* **2011**, *14* (5), 573−584.
(87) Liu, H.; Abecasis, G. R.; Heath, S. C.; Knowles, A.; Demars, S.; Chen, Y. J.; Roos, J. L.; Rapoport, J. L.; Gogos, J. A.; Karayiorgou, M. Genetic variation in the 22q11 locus and susceptibility to schizophrenia. *Proc. Natl. Acad. Sci. U.S.A.* **2002**, *99* (26), 16859−16864.
(88) Shifman, S.; Bronstein, M.; Sternfeld, M.; Pisante-Shalom, A.; Lev-Lehman, E.; Weizman, A.; Reznik, I.; Spivak, B.; Grisaru, N.; Karp, L.; Schiffer, R.; Kotler, M.; Strous, R. D.; Swartz-Vanetik, M.; Knobler, H. Y.; Shinar, E.; Beckmann, J. S.; Yakir, B.; Risch, N.; Zak, N. B.; Darvasi, A. A highly significant association between a COMT haplotype and schizophrenia. *Am. J. Hum. Genet.* **2002**, *71* (6), 1296−1302.
(89) Egan, M. F.; Goldberg, T. E.; Kolachana, B. S.; Callicott, J. H.; Mazzanti, C. M.; Straub, R. E.; Goldman, D.; Weinberger, D. R. Effect of COMT Val108/158 Met genotype on frontal lobe function and risk for schizophrenia. *Proc. Natl. Acad. Sci. U.S.A.* **2001**, *98* (12), 6917−6922.
(90) Fukui, N.; Suzuki, Y.; Sugai, T.; Watanabe, J.; Ono, S.; Tsuneyama, N.; Someya, T. Promoter variation in the catechol-O-methyltransferase gene is associated with remission of symptoms during fluvoxamine treatment for major depression. *Psychiatry Res.* **2014**, *218* (3), 353−355.
(91) Curley, A. A.; Eggan, S. M.; Lazarus, M. S.; Huang, Z. J.; Volk, D. W.; Lewis, D. A. Role of glutamic acid decarboxylase 67 in regulating cortical parvalbumin and GABA membrane transporter 1 expression: Implications for schizophrenia. *Neurobiol. Disease* **2013**, *50*, 179−186.
(92) Sarnyai, Z.; Alsaif, M.; Bohn, S.; Ernst, A.; Guest, P. C.; Hradetzky, E.; Kluge, W.; Stelzhammer, V.; Wesseling, H. Behavioral and molecular biomarkers in translational animal models for neuropsychiatric disorders. *Int. Rev. Neurobiol.* **2011**, *101*, 203−238.
(93) Schobel, S. A.; Chaudhury, N. H.; Khan, U. A.; Paniagua, B.; Styner, M. A.; Asllani, I.; Inbar, B. P.; Corcoran, C. M.; Lieberman, J. A.; Moore, H.; Small, S. A. Imaging patients with psychosis and a mouse model establishes a spreading pattern of hippocampal dysfunction and implicates glutamate as a driver. *Neuron* **2013**, *78* (1), 81−93.
(94) Stan, A. D.; Ghose, S.; Zhao, C.; Hulsey, K.; Mihalakos, P.; Yanagi, M.; Morris, S. U.; Bartko, J. J.; Choi, C.; Tamminga, C. A., Magnetic resonance spectroscopy and tissue protein concentrations together suggest lower glutamate signaling in dentate gyrus in schizophrenia. *Mol. Psychiatry* **2014**, 10.1038/mp.2014.54.
(95) Paul, I. A.; Skolnick, P. Glutamate and depression: clinical and preclinical studies. *Ann. N.Y. Acad. Sci.* **2003**, *1003*, 250−272.
(96) Schubert, K. O.; Focking, M.; Prehn, J. H. M.; Cotter, D. R. Hypothesis review: are clathrin-mediated endocytosis and clathrin-dependent membrane and protein trafficking core pathophysiological processes in schizophrenia and bipolar disorder? *Mol. Psychiatry* **2012**, *17* (7), 669−681.
(97) Gottschalk, M. G.; Wesseling, H.; Guest, P. C.; Bahn, S. *Int. J. Neuropsychopharmacol.* **2014**, DOI: 10.1093/ijnp/pyu019.
(98) Zhu, G.; Okada, M.; Uchiyama, D.; Ohkubo, T.; Yoshida, S.; Kaneko, S. Hyperactivity of endoplasmic reticulum associated exocytosis mechanism contributes to acute phencyclidine intoxication. *J. Pharmacol. Sci.* **2004**, *95* (2), 214−227.
(99) Pickering, C.; Ericson, M.; Soderpalm, B. Chronic phencyclidine increases synapsin-1 and synaptic adaptation proteins in the medial prefrontal cortex. *ISRN Psychiatry* **2013**, 620361.

DOI: 10.1021/pr5009493
J. Proteome Res. 2015, 14, 411−421